MAP BASED DIFFERENTIAL DETECTORS FOR COMPRESSED UWB IMPULSE RADIO SIGNALS

*Shahzad Gishkori, Geert Leus**

Faculty of EEMCS
Delft University of Technology
Delft, The Netherlands

Vincenzo Lottici

Department of Information Engineering
University of Pisa
Pisa, Italy

ABSTRACT

We propose maximum a posteriori (MAP) based noncoherent differential detector for ultra-wideband (UWB) impulse radio (IR) signals, received at a sub-Nyquist sampling rate. We build our detector for a Laplacian distributed multipath channel, which models sparsity. Our MAP based detector outperforms differential detectors based on other state-of-the-art approaches from a practical point of view. Our work highlights the critical role of different measurement matrices for the compressed differential detectors in general and the MAP based compressed differential detectors in particular.

Index Terms— Ultra-wideband impulse radio, differential detection, compressive sampling, LASSO, MAP, Laplacian distribution

1. INTRODUCTION

Ultra-wideband (UWB) impulse radio (IR) is a signaling scheme that is potentially suitable for low-power short-range communications due to a number of salient features such as a high user capacity, fine timing resolution, low probability of interception and detection etc. [1]. Rich multipath propagation, however, makes each transmitted pulse appear at the receiver as hundreds of echoes. Although Rake receivers allow to collect most of the energy conveyed by the multipath components, they require a large number of fingers together with an intensive computational load and high sampling rate to perform channel estimation, which belies the major requirement of simple transceiver devices. Noncoherent receivers have been proposed, as suboptimal yet effective alternatives, in order to avoid the difficult channel estimation task, in the form of autocorrelation based receivers (AcRs) [2], such as transmitted reference (TR), where a reference pulse is transmitted together with the data pulse, and differential detection (DD), which employs differential encoding. The detection performance of DD schemes can be further improved by adopting the multi-symbol DD approach (MSDD) [3]. But even then, for an all-digital implementation, they are all affected by the basic issue of requiring high-rate analog-to-digital converters (ADCs).

The compressive sampling (CS) concept is a powerful way to reduce the sampling rate of sparse signals much below the Nyquist-rate without incurring large performance degradations [4]-[5]. The sampling rate is reduced by means of a few random projections in the analog domain, and then, the signal is recovered from this low-dimensional representation. Now, exploiting the fact that the received UWB signal can be considered to be sparse in the time domain, the CS-based approach can be useful for data detection as proposed in [6] for alternating direction method of multipliers (ADMoM) based compressed noncoherent receivers for differentially encoded UWB signals.

Focusing on noncoherent receivers, we propose in this paper a maximum a posteriori (MAP) based DD for the compressed received symbols. We present a joint model for two consecutive received symbols. We do not require channel estimation, nor the transmission of pilot symbols as in [7] and [8], respectively. We develop a compressed-rate MAP DD assuming a Laplacian distributed channel.

Notations: Matrices are in upper case bold while column vectors are in lower case bold, $\mathbf{I}_N$ is the identity matrix of size $N \times N$, $|\mathbf{A}|$ is the determinant of the matrix $\mathbf{A}$, $(\cdot)^T$ is transpose, $(\cdot)^+$ is pseudo-inverse, $\otimes$ stands for the Kronecker product, diag$\{\cdot\}$ presents a block diagonal matrix having the arguments along its main diagonal, $\hat{x}$ is the estimate of x, E$\{\cdot\}$ denotes expectation, $P(\cdot)$ and $p(\cdot)$ represent probability distribution and probability density function (pdf), respectively, $\triangleq$ defines an entity, $\|\mathbf{a}\|_p = (\sum_{i=0}^{N-1} \left|[\mathbf{a}]_i\right|^p)^{1/p}$ is the ℓ_p norm of $\mathbf{a}$ and sign(x) is the sign function which takes values -1 and 1 depending on the polarity of the element x.

2. SIGNAL MODEL

In the adopted IR-UWB signal model, each symbol is conveyed by a pulse $q(t)$ of duration T_q much less than the symbol interval T_s, i.e., $T_q \ll T_s$ [1]. The transmitted signal composed of a block of Q symbols takes the form

$$s(t) = \sum_{k=0}^{Q-1} b_k q(t - kT_s) \tag{1}$$

where $b_k \in \{\pm 1\}$ are the differentially encoded transmitted symbols, i.e., $b_k = b_{k-1}a_k$, $a_k \in \{\pm 1\}$ being the information symbols. As a reference transmitted symbol, we take $b_{-1} = 1$ without loss of generality. The signal travels through a slow-fading multipath channel which is assumed to be time-invariant within the interval of Q consecutive symbols, and with a delay spread smaller than T_s, so that inter symbol interference (ISI) is avoided. Let $g(t) \triangleq \sum_{l=0}^{L-1} \alpha_l \delta(t - \tau_l)$ represent the channel impulse response (CIR) with L paths, where α_l and τ_l are the gain and path delay of the lth path, respectively. The received signal $r(t)$ can then be written

*This work is supported in part by NWO-STW under the VICI program (project 10382).

[1] Generalizations of the proposed framework to signaling based on multiple frames to comply with the FCC power spectral density requirements can be easily performed. For the sake of simplicity, this model will not be addressed.

as

$$r(t) = \underbrace{\sum_{k=0}^{Q-1} b_k h(t - kT_s)}_{\triangleq x(t)} + v(t) \quad (2)$$

where $h(t) \triangleq \sum_{l=0}^{L-1} \alpha_l q(t - \tau_l)$ is the received pulse, and $v(t)$ is the zero-mean additive white Gaussian noise component with variance σ_v^2. Denoting with $1/T = N/T_s$ the Nyquist sampling rate, the received signal in its sampled version can be written as $\mathbf{r} \triangleq [\mathbf{r}_0^T, \mathbf{r}_1^T, \cdots, \mathbf{r}_{Q-1}^T]^T$ where $\mathbf{r}_k \triangleq [r(kT_s), r(kT_s + T), \cdots, r(kT_s + NT - T)]^T$ collects the N Nyquist-rate samples corresponding to the kth symbol. In view of (2), it can be obtained, $\mathbf{r}_k = \mathbf{x}_k + \mathbf{v}_k$, where $\mathbf{x}_k = b_k \mathbf{h}$, $\mathbf{h} \triangleq [h(0), h(T), \cdots, h(NT - T)]^T$ is the sampled CIR whose entries are modeled as independent and identically distributed (i.i.d.) Laplacian random variables, and $\mathbf{v}_k \triangleq [v(kT_s), v(kT_s+T), \cdots, v(kT_s+NT-T)]^T$ is a zero-mean Gaussian random vector with covariance matrix $\mathrm{E}\{\mathbf{v}_k \mathbf{v}_k^T\} = \sigma_v^2 \mathbf{I}_N$. Given the sparse nature of $\mathbf{x}_k$ (due to the sparse channel), most of its components are zero or negligible and thus, according to the CS framework theory [4, 5], it can be represented by M linear measurements, with $M \ll N$. This process takes place in the analog domain but for the sake of convenience, we represent these operations performed on the Nyquist rate samples of $r(t)$. Hence, the compressed received signal within one symbol can be expressed as, $\mathbf{y}_k = \mathbf{\Phi}_k \mathbf{r}_k = \mathbf{\Phi}_k \mathbf{x}_k + \boldsymbol{\xi}_k$, where the $M \times N$ matrix $\mathbf{\Phi}_k$ is the measurement matrix (which satisfies the restricted isometry property (RIP) [5]) at time instant k, $\boldsymbol{\xi}_k \triangleq \mathbf{\Phi}_k \mathbf{v}_k$ is the noise component and $M \ll N$. The signal model for two consecutive received symbol waveforms sampled at compressed rate can be formulated as

$$\mathbf{y} = \mathbf{\Phi}(\mathbf{b} \otimes \mathbf{I}_N)\mathbf{h} + \boldsymbol{\xi} \quad (3)$$

where $\mathbf{y} \triangleq [\mathbf{y}_k^T, \mathbf{y}_{k+1}^T]^T$, $\mathbf{b} \triangleq [b_k, b_{k+1}]^T$ and $\boldsymbol{\xi} \triangleq [\boldsymbol{\xi}_k^T, \boldsymbol{\xi}_{k+1}^T]^T$, whereas $\mathbf{\Phi} \triangleq \mathrm{diag}\{\mathbf{\Phi}_k, \mathbf{\Phi}_{k+1}\}$, with $\mathbf{\Phi}_{k+l}$, being the $M \times N$ measurement matrix satisfying $\mathbf{\Phi}_{k+l}\mathbf{\Phi}_{k+l}^T = \mathbf{I}_M$, $l = 0, 1$.

3. ℓ_1-NORM BASED RECONSTRUCTION AND DETECTION

The conventional Nyquist-rate DD (NDD) can be written as

$$\hat{a}_{k+1}^{(\mathrm{NDD})} = \mathrm{sign}\left(\arg\min_a \left\{\|\mathbf{r}_k - a\mathbf{r}_{k+1}\|_2^2\right\}\right) \quad (4)$$

whereas the detector for the compressed symbols directly, i.e., the direct compressed differential detector (DC-DD) can be written as

$$\hat{a}_{k+1}^{(\mathrm{DC-DD})} = \mathrm{sign}\left(\arg\min_a \left\{\|\mathbf{y}_k - a\mathbf{y}_{k+1}\|_2^2\right\}\right). \quad (5)$$

Instead of directly correlating the received compressed symbols as in (5), one may want to reconstruct the original symbols from their compressed measurements and then detect the encoded information. There can be two approaches to this end, either to separately reconstruct the symbols from their compressed version and then carry out detection, i.e., separate compressed DD (SC-DD), or to carry out the reconstruction and detection process jointly, i.e., joint compressed DD (JC-DD). Furthermore, given the sparse nature of the received symbols, an ℓ_1-norm based reconstruction can be employed. For example, the least absolute shrinkage and selection operator (LASSO) [9] adopts a regularization term based on the ℓ_1 norm and reconstructs the symbols as

$$\hat{\mathbf{x}}_{k+l} = \arg\min_{\mathbf{x}_{k+l}} \left\{\|\mathbf{y}_{k+l} - \mathbf{\Phi}_{k+l}\mathbf{x}_{k+l}\|_2^2 + \lambda \|\mathbf{x}_{k+l}\|_1\right\} \quad (6)$$

where λ is the Lagrangian constant and $l = 0, 1$. The SC-DD would then involve correlating these reconstructed symbols. In case of JC-DD, following cost function has to be minimized over $\mathbf{x}_k$, $\mathbf{x}_{k+1}$ and a_{k+1}

$$\mathcal{C} \triangleq \sum_{l=0}^{1} \left[\|\mathbf{y}_{k+l} - \mathbf{\Phi}_{k+l}\mathbf{x}_{k+l}\|_2^2 + \lambda \|\mathbf{x}_{k+l}\|_1\right] + \alpha \|\mathbf{x}_k - a_{k+1}\mathbf{x}_{k+1}\|_2^2 \quad (7)$$

where λ is again the Lagrangian constant and α is a weight constant. The exact solutions to both the SC-DD and DC-DD (under the rubric of differential elastic net (DEN)), based on pathwise coordinate descent methods [10], are provided in [11]. We shall compare the performance of these methods with our compressed MAP based DD.

4. COMPRESSED-RATE MAP DETECTOR

From (3) the compressed-rate MAP differential detector (C-MAP-DD) is given by

$$\hat{\mathbf{b}} = \arg\max_{\mathbf{b}} \{p(\mathbf{y}|\mathbf{b})P(\mathbf{b})\} \quad (8)$$

where $P(\mathbf{b})$ is the a priori distribution of the transmitted symbols $\mathbf{b}$. From (3), it can be seen that $p(\mathbf{y}|\mathbf{b})$ is the convolution of the joint pdfs of Laplacian and normally distributed random variables. This reflects the complication of obtaining a MAP based DD for the compressed signals. In this paper, we circumvent this problem by giving $\mathbf{h}$ a rather amenable form. A Laplacian distributed random variable can be represented as a normal distributed random variable but with a stochastic variance [12]. We represent $\mathbf{h}$ as the product between a Rayleigh and a normal distributed random variable, i.e., $\mathbf{h} = \rho\mathbf{n}$, where the pdf of ρ is, $p(\rho) = \rho e^{-\rho^2/2}$, and $\mathbf{n}$ is a zero-mean joint normal random vector with covariance matrix $\mathbf{C}_\mathbf{n} = \mathbf{I}_N$. So $\mathbf{y} = \mathbf{\Phi}(\mathbf{b} \otimes \mathbf{I}_N)\rho\mathbf{n} + \boldsymbol{\xi}$, and the pdf of $\mathbf{y}$ given $\mathbf{b}$ can be written as

$$p(\mathbf{y}|\mathbf{b}) = \int_0^\infty p(\mathbf{y}|\mathbf{b}, \rho)p(\rho)d\rho \quad (9)$$

where $p(\mathbf{y}|\mathbf{b}, \rho)$ is the zero-mean joint normal distribution, i.e.,

$$p(\mathbf{y}|\mathbf{b}, \rho) = \frac{1}{\pi^{2M}\left|\mathbf{C}_{\mathbf{y}|\mathbf{b},\rho}\right|} e^{-\mathbf{y}^T \mathbf{C}_{\mathbf{y}|\mathbf{b},\rho}^{-1}\mathbf{y}}. \quad (10)$$

Taking into account the assumption, $\mathbf{\Phi}\mathbf{\Phi}^T = \mathbf{I}_{2M}$, the covariance matrix $\mathbf{C}_{\mathbf{y}|\mathbf{b},\rho}$ can be written as

$$\begin{aligned}\mathbf{C}_{\mathbf{y}|\mathbf{b},\rho} &= \mathrm{E}\{[\mathbf{\Phi}(\mathbf{b} \otimes \mathbf{I}_N)\rho\mathbf{n} + \boldsymbol{\xi}]\,[\mathbf{\Phi}(\mathbf{b} \otimes \mathbf{I}_N)\rho\mathbf{n} + \boldsymbol{\xi}]^T\} \\ &= \sigma_v^2 \mathbf{I}_{2M} + \rho^2 \mathbf{\Phi}(\mathbf{b}\mathbf{b}^T \otimes \mathbf{I}_N)\mathbf{\Phi}^T \end{aligned} \quad (11)$$

whereas its inverse can be computed from the binomial inverse theorem as

$$\begin{aligned}\mathbf{C}_{\mathbf{y}|\mathbf{b},\rho}^{-1} &= \left[\sigma_v^2 \mathbf{I}_{2M} + \rho^2 \mathbf{\Phi}(\mathbf{b}\mathbf{b}^T \otimes \mathbf{I}_N)\mathbf{\Phi}^T\right]^{-1} \\ &= \frac{1}{\sigma_v^2}\left[\mathbf{I}_{2M} - \frac{\rho^2}{\sigma_v^2}\mathbf{\Phi}(\mathbf{b} \otimes \mathbf{I}_N)\mathbf{\Sigma}^{-1}(\mathbf{b} \otimes \mathbf{I}_N)^T\mathbf{\Phi}^T\right] \end{aligned} \quad (12)$$

where

$$\begin{aligned}\boldsymbol{\Sigma} &\triangleq \mathbf{I}_N + \frac{\rho^2}{\sigma_v^2}(\mathbf{b}\otimes\mathbf{I}_N)^T\boldsymbol{\Phi}^T\boldsymbol{\Phi}(\mathbf{b}\otimes\mathbf{I}_N)\\ &= \mathbf{I}_N + \frac{\rho^2}{\sigma_v^2}\left(\boldsymbol{\Phi}_k^T\boldsymbol{\Phi}_k + \boldsymbol{\Phi}_{k+1}^T\boldsymbol{\Phi}_{k+1}\right). \qquad (13)\end{aligned}$$

Finally, using the Sylvester theorem, the determinant of $\mathbf{C}_{\mathbf{y}|\mathbf{b},\rho}$ is given by

$$\begin{aligned}\left|\mathbf{C}_{\mathbf{y}|\mathbf{b},\rho}\right| &= \left|\sigma_v^2\mathbf{I}_{2M} + \rho^2\boldsymbol{\Phi}(\mathbf{b}\mathbf{b}^T\otimes\mathbf{I}_N)\boldsymbol{\Phi}^T\right|\\ &= \sigma_v^{4M}\left|\mathbf{I}_N + \frac{\rho^2}{\sigma_v^2}(\mathbf{b}\otimes\mathbf{I}_N)^T\boldsymbol{\Phi}^T\boldsymbol{\Phi}(\mathbf{b}\otimes\mathbf{I}_N)\right|, \qquad (14)\end{aligned}$$

or equivalently from (13),

$$\left|\mathbf{C}_{\mathbf{y}|\mathbf{b},\rho}\right| = \sigma_v^{4M}\left|\mathbf{I}_N + \frac{\rho^2}{\sigma_v^2}\left(\boldsymbol{\Phi}_k^T\boldsymbol{\Phi}_k + \boldsymbol{\Phi}_{k+1}^T\boldsymbol{\Phi}_{k+1}\right)\right| \qquad (15)$$

which is independent of $\mathbf{b}$. Now exploiting the assumption that $\mathbf{b}$ is uniformly distributed, maximizing $p(\mathbf{y}|\mathbf{b})P(\mathbf{b})$ over $\mathbf{b}$ is same as maximizing $p(\mathbf{y}|\mathbf{b})$. Now from (9), if the maximum of $p(\mathbf{y}|\mathbf{b},\rho)$ over $\mathbf{b}$ for each value of ρ is independent of ρ then that is also the maximum of $p(\mathbf{y}|\mathbf{b})$. Finding the maximum of $p(\mathbf{y}|\mathbf{b},\rho)$ over $\mathbf{b}$ means maximizing the exponent in (10) or equivalently, the function obtained after dropping immaterial addends independent of $\mathbf{b}$:

$$\Psi_{\mathrm{C}}(\mathbf{y}|\mathbf{b},\rho) \triangleq \mathbf{y}^T\boldsymbol{\Phi}(\mathbf{b}\otimes\mathbf{I}_N)\boldsymbol{\Sigma}^{-1}(\mathbf{b}\otimes\mathbf{I}_N)^T\boldsymbol{\Phi}^T\mathbf{y} \qquad (16)$$

However this function is still dependent on ρ due to the presence of $\boldsymbol{\Sigma}^{-1}$. Such a matrix inverse can be computed by exploiting the eigenvalue decomposition (EVD) of the $N\times N$ semi-positive definite matrix $\boldsymbol{\Phi}_k^T\boldsymbol{\Phi}_k + \boldsymbol{\Phi}_{k+1}^T\boldsymbol{\Phi}_{k+1}$ given by $\mathbf{Q}\boldsymbol{\Omega}\mathbf{Q}^T$, with $\boldsymbol{\Omega}$ having non-negative elements along its main diagonal and $\mathbf{Q}\mathbf{Q}^T = \mathbf{I}_N$. Thus, replacing the EVD into (16) yields

$$\Psi_{\mathrm{C}}(\mathbf{y}|\mathbf{b},\rho) \triangleq \mathbf{y}^T\boldsymbol{\Phi}(\mathbf{b}\otimes\mathbf{I}_N)\mathbf{Q}\boldsymbol{\Omega}_\Sigma\mathbf{Q}^T(\mathbf{b}\otimes\mathbf{I}_N)^T\boldsymbol{\Phi}^T\mathbf{y}. \qquad (17)$$

where $\boldsymbol{\Omega}_\Sigma = \left(\mathbf{I}_N + \frac{\rho^2}{\sigma_v^2}\boldsymbol{\Omega}\right)^{-1}$. Now, taking into account that the diagonal matrix $\boldsymbol{\Omega}_\Sigma$ has entries which are strictly positive and less than unity, (17) can be approximated by its upper bound (independent of ρ):

$$\Upsilon_{\mathrm{C}}(\mathbf{y}|\mathbf{b}) \triangleq \mathbf{y}^T\boldsymbol{\Phi}(\mathbf{b}\otimes\mathbf{I}_N)(\mathbf{b}\otimes\mathbf{I}_N)^T\boldsymbol{\Phi}^T\mathbf{y}, \qquad (18)$$

which can be properly rearranged as

$$\Upsilon_{\mathrm{C}}(\mathbf{y}|\mathbf{b}) = b_{k+1}b_k\mathbf{y}_{k+1}^T\boldsymbol{\Phi}_{k+1}\boldsymbol{\Phi}_k^T\mathbf{y}_k. \qquad (19)$$

Thus, in view of the differential encoding rule $a_{k+1} = b_{k+1}b_k$, we end up with the following approximate information decoding rule

$$\hat{a}_{k+1}^{(\mathrm{C-MAP-DD})} = \mathrm{sign}\left(\mathbf{y}_{k+1}^T\boldsymbol{\Phi}_{k+1}\boldsymbol{\Phi}_k^T\mathbf{y}_k\right). \qquad (20)$$

Some remarks about the C-MAP-DD scheme can be of interest.

1. The ordinary least squares DD (OLS-DD) estimate of the information symbol a_{k+1} is obtained as

$$\hat{a}_{k+1}^{\mathrm{OLS-DD}} = \mathrm{sign}\left[(\boldsymbol{\Phi}_{k+1}^+\mathbf{y}_{k+1})^T(\boldsymbol{\Phi}_k^+\mathbf{y}_k)\right] \qquad (21)$$

where $l = 0, 1$. Since the measurement matrices have orthonormal rows, it can be shown that $\boldsymbol{\Phi}_{k+l}^+ = \boldsymbol{\Phi}_{k+l}^T, l = 0, 1$. Therefore, we get

$$(\boldsymbol{\Phi}_{k+1}^+\mathbf{y}_{k+1})^T(\boldsymbol{\Phi}_k^+\mathbf{y}_k) = \mathbf{y}_{k+1}^T\boldsymbol{\Phi}_{k+1}\boldsymbol{\Phi}_k^T\mathbf{y}_k, \qquad (22)$$

from which we may argue that the OLS-DD coincides with the C-MAP-DD.

2. Assuming $\boldsymbol{\Phi}_{k+1} = \boldsymbol{\Phi}_k$ and exploiting $\boldsymbol{\Phi}_k\boldsymbol{\Phi}_k^T = \mathbf{I}_M$, we obtain from (20)

$$\mathbf{y}_{k+1}^T\boldsymbol{\Phi}_{k+1}\boldsymbol{\Phi}_k^T\mathbf{y}_k = \mathbf{y}_{k+1}^T\mathbf{y}_k \qquad (23)$$

which means that, whenever the measurement matrices are time-invariant, the C-MAP-DD coincides with the DC-DD.

3. If the measurement matrices are orthogonal to each other, i.e., $\boldsymbol{\Phi}_k\boldsymbol{\Phi}_l^T = \mathbf{0}_M$ if $\boldsymbol{\Phi}_k \neq \boldsymbol{\Phi}_l$, then we can see from (20) that the C-MAP-DD does not exist.

5. SIMULATION RESULTS

The transmitted signal consists of differentially-encoded symbols, each conveyed by an ultra short pulse traveling through a Laplacian distributed propagation channel. For the sake of simplicity, we assume that the channel response includes the effect of the shaping filters at both the transmitter and receiver sides. The received symbol waveform sampled at Nyquist rate contains $N = 32$ samples and it is compressed with a compression ratio $\mu \triangleq M/N$, resulting in $M < N$ samples. The measurement matrix $\boldsymbol{\Phi}_k$ has zero-mean unit-variance i.i.d. normal entries with orthonormalized rows, and can be chosen within consecutive symbols to be the same ($\boldsymbol{\Phi}_k = \boldsymbol{\Phi}_{k+1}$) or different from each other ($\boldsymbol{\Phi}_k \neq \boldsymbol{\Phi}_{k+1}$).

Figs. 1-3 quantify the BER detection performance as a function of the E_b/N_0 ratio, assuming that the measurement matrices are chosen to be the same or different from each other, respectively. While the reference NDD works at Nyquist-rate, all the other schemes adopt a compression ratio of $\mu = 0.5$ or $\mu = 0.75$. Furthermore, for the sake of comparisons, we plot the complete C-MAP-DD (8), to verify its approximate in (20).

We see in Fig. 1 that for the case when the measurement matrices are the same (i.e., $\boldsymbol{\Phi}_k = \boldsymbol{\Phi}_{k+1}$), all detectors perform reasonably well. The DC-DD overlaps with the C-MAP-DD, according to what we observed in remark 2 of Sect. 4, along with the JC-DD whereas the SC-DD lags behind by 1 dB. Increasing the compression ratio to $\mu = 0.75$ decreases the performance gap between the NDD and the compression based detectors, which shows the trade-off between performance and compression ratio. The results of Fig. 2, with different measurement matrices (i.e., $\boldsymbol{\Phi}_k \neq \boldsymbol{\Phi}_{k+1}$), show a considerable advantage of the C-MAP-DD and JC-DD over the DC-DD and SC-DD, with the C-MAP-DD having an edge over the JC-DD. It should be noted that the overall performance of compressed detectors is not better than the case when the measurement matrices are the same. Further, from both Fig. 1 and Fig. 2, it is apparent that the performance of the OLS-DD equals that offered by the C-MAP-DD, as expected from remark 1 of Sect. 4. Fig. 3 shows the BER performance of compressed detectors (C-MAP-DD, SC-DD and JC-DD) for the case when the measurement matrices are orthogonal to each other (i.e., $\boldsymbol{\Phi}_k \perp \boldsymbol{\Phi}_{k+1}$). It can be seen that C-MAP-DD completely misses the detection as noted in remark 3 of Sect. 4. It seems that due to the compression by orthogonal matrices, the MAP is not able to recover the encoded information from the joint model. The ℓ_1-norm based methods perform slightly better because, in a sense, they treat each symbol individually for reconstruction. But their performance is also limited by the compression ratio μ. Since we cannot create mutually orthogonal measurement matrices (with orthogonal rows in each matrix individually), for $\mu > 0.5$ i.e., $M > N/2$, the performance of the ℓ_1-norm based methods cannot be improved further than what is seen in Fig. 3. Thus in practice such matrices may not be used at all. Therefore, we can say that for all practical scenarios, C-MAP-DD is a good option.

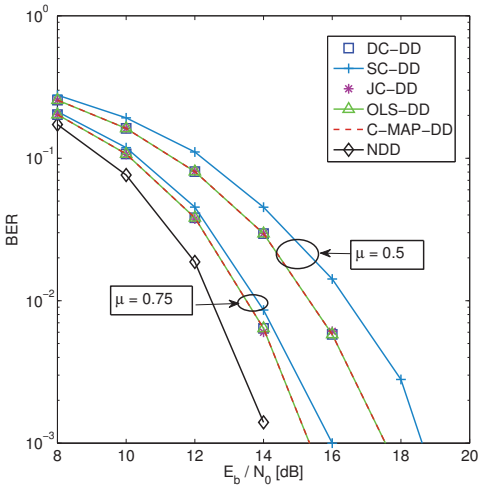

Fig. 1. BER comparison for different detection methods with $\mathbf{\Phi}_k = \mathbf{\Phi}_{k+1}$ and compression ratio $\mu = 0.5, 0.75$.

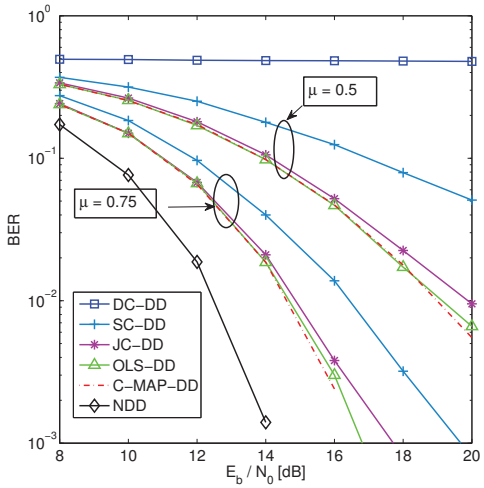

Fig. 2. BER comparison for different detection methods with $\mathbf{\Phi}_k \neq \mathbf{\Phi}_{k+1}$ and compression ratio $\mu = 0.5, 0.75$.

6. CONCLUSIONS

In this paper, the compressive sampling framework has been applied to differentially encoded UWB signals which reduces the sampling rate as well as offers the ability to carry out differential detection in the digital domain. We have derived a compressed MAP based differential detector. It offers an alternative to ℓ_1-norm based differential detection. For the compressed differential detectors, we have seen that the performance is heavily influenced by the type of measurement matrices that are chosen. It has been shown that for practical scenarios of the measurement matrices, the MAP based compressed differential detector yields a good choice.

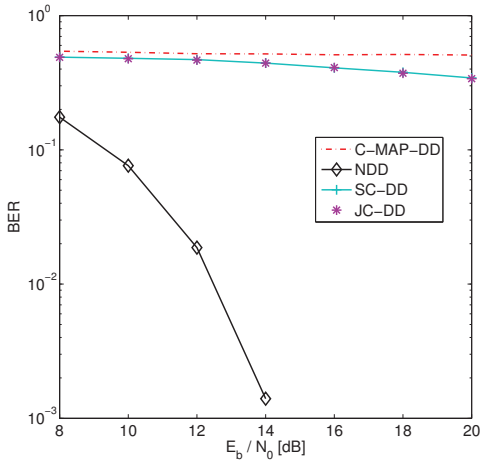

Fig. 3. BER comparison for different detection methods with $\mathbf{\Phi}_k \perp \mathbf{\Phi}_{k+1}$ and compression ratio $\mu = 0.5$.

7. REFERENCES

[1] M. Z. Win and R. A. Scholtz, "Impulse radio: how it works," *IEEE Communication Letters*, vol. 2, no. 2, pp. 36-38, Feb. 1998.

[2] K. Witrisal, G. Leus, G. Janssen, M. Pausini, F. Troesch, T. Zasowski, and J. Romme, "Noncoherent ultra-wideband systems," *IEEE Signal Processing Magazine*, vol. 26, no. 4, pp. 48-66, July 2009.

[3] V. Lottici, Z. Tian, "Multiple symbol differential detection for UWB communications," *IEEE Transaction on Wireless Communication*, vol. 7, no. 5, pp. 1656-1666, 2008.

[4] David L. Donoho, "Compressed sensing," *IEEE Transaction on Information Theory*, vol. 52, no. 4,April 2006.

[5] E. Candès, J. Romberg and T. Tao, "Robust uncertainty principles: exact signal reconstruction from highly incomplete frequency information," *IEEE Transaction on Information Theory*, vol. 52, no. 2, pp. 489-509, February 2006.

[6] S. Gishkori, G. Leus and V. Lottici, "Compressive sampling based differential detection of ultra wideband signals," *Proc. IEEE PIMRC 2010*, Sep. 2010.

[7] A. Oka and L. Lampe, "A compressed sensing receiver for uwb impulse radio in bursty applications like wireless sensor networks," *Elsevier Physical Communication*, vol. 2, no. 4, pp. 248-264, Dec. 2009.

[8] Z. Wang, G.R. Arce, J.L. Paredes and B.M. Sadler, "Compressed detection for ultra-wideband impulse radio," *IEEE SPAWC*, 2007.

[9] R. Tibshirani, "Regression shrinkage and selection via the lasso", *Journal of the Royal Statistical Society*, series B, vol. 58, no. 1, pp. 267-288, 1996.

[10] J. Friedman, T. Hastie, H. Höfling and R. Tibshirani, "Pathwise coordinate optimization," *The annals of Applied Statistics*, vol. 1, no. 2, pp. 302-332, Aug. 2007.

[11] S. Gishkori, G. Leus and V. Lottici, "Compressive sampling based differential detection for uwb impulse radio signals," *Elsevier Physical Communication*. To appear.

[12] S. Kotz, T.J. Kozubowski, K. Podgrski, *The Laplace distribution and generalizations*, Birkhauser, Boston, 2001.